Chemical Science

ROYAL SOCIETY OF CHEMISTRY

EDGE ARTICLE

View Article Online
View Journal | View Issue

Cite this: *Chem. Sci.*, 2025, **16**, 21394

All publication charges for this article have been paid for by the Royal Society of Chemistry

Received 17th July 2025
Accepted 6th October 2025

DOI: 10.1039/d5sc05320j

rsc.li/chemical-science

Catalytic asymmetric synthesis of indole-based atropisomers bearing silicon-stereogenic centers

Si-Yi Liu,†[a] Zi-Qi Zhu,†*[a] Fei-Xiao Chen,[b] Ni-Na Feng,[a] Shao-Fei Ni*[bc] and Feng Shi *[ad]

The first diastereo- and enantioselective synthesis of indole-based atropisomers bearing Si-stereogenic centers has been established *via* the strategy of catalytic asymmetric reductive silylation. By this strategy, a wide range of indole-based atropisomers bearing Si-stereogenic centers were synthesized in moderate to good yields with overall excellent enantioselectivities and good diastereoselectivities (up to 87% yield, 94% ee, 7.3 : 1 dr). This work not only provides a new strategy for catalytic asymmetric synthesis of atropisomers bearing Si-stereogenic centers, but also has realized the first catalytic asymmetric synthesis of indole-based atropisomers with a Si-stereogenic center, which will add an important member to the family of indole-based atropisomers bearing multiple chiral elements. Moreover, this work also presents the first catalytic asymmetric reductive silylation of indole scaffolds, which adds new content to enantioselective C–Si bond formation.

Introduction

Due to the unique features of atropisomerism, catalytic asymmetric synthesis of atropisomers has triggered massive attention from the chemical science community.[1,2] In particular, catalytic asymmetric synthesis of atropisomers bearing multiple stereogenic elements has recently become a frontier area of research[3] owing to the promising applications of such atropisomers in developing chiral ligands[4] and discovering bioactive molecules (Fig. 1a).[5] However, as summarized in Fig. 1b, despite the rapid growth of this research area, most of the transformations are focused on catalytic asymmetric synthesis of atropisomers bearing carbon-stereogenic centers (more than eighty reports),[3c,d,5–7] while catalytic asymmetric synthesis of atropisomers bearing heteroatom-stereogenic centers is rather underdeveloped, and only around fifteen reports appeared, including catalytic asymmetric synthesis of atropisomers bearing P-, S- and Si-stereogenic centers.[8–11] Particularly noteworthy is that only two reports systematically investigated the catalytic asymmetric synthesis of atropisomers bearing Si-stereogenic centers,[10] which can be ascribed to the difficulties in enantioselectively constructing Si-stereogenic centers.[12–14] For example, compared with C, P, and S atoms, the larger atomic radius and lower electronegativity of Si decrease its ability to form strong π-bonds and lead to an unstable sp^2-hybridized state of Si, thus resulting in very limited strategies for constructing Si-stereogenic centers.[12f]

As shown in Fig. 1c, there are only very limited reports on catalytic asymmetric synthesis of atropisomers bearing Si-stereogenic centers. In 2021, Gu's group applied the desymmetrization strategy in catalytic asymmetric ring-opening/acylation of torsionally strained silafluorenes under the catalysis of an Rh/chiral ligand,[10a] synthesizing biaryl atropisomers bearing Si-stereogenic centers *via* the cleavage of Si–C bonds (eqn (1)). In the same year, He's group reported another strategy of catalytic asymmetric dehydrogenative coupling under the catalysis of an Rh/chiral ligand, constructing bridged biaryl atropisomers bearing Si-stereogenic centers (eqn (2)).[10b] In spite of these elegant approaches, the established strategies rely on using presilylated biaryl precursors as substrates, and the activation of C–Si/C–H bonds necessitates noble metal catalysis. Moreover, the constructed scaffolds are confined to biaryl atropisomers bearing Si-stereogenic centers. Therefore, the remaining challenges in this field mainly include (1) developing new strategies for catalytic asymmetric synthesis of atropisomers bearing Si-stereogenic centers; (2) designing a new class of atropisomers bearing Si-stereogenic centers and their effective synthetic methods; and (3) controlling the enantioselectivity and diastereoselectivity of atropisomers bearing Si-stereogenic centers.

To tackle these challenges, based on our understanding of chiral indole chemistry,[15] we conceive designing a new class of

[a]*School of Petrochemical Engineering, Institute of Functional Heterocycles, School of Materials Science & Engineering, Changzhou University, Changzhou, 213164, China. E-mail: fshi@jsnu.edu.cn; zzq@cczu.edu.cn*

[b]*College of Chemistry & Chemical Engineering, Shantou University, Shantou, 515063, China. E-mail: sfni@stu.edu.cn*

[c]*Chemistry and Chemical Engineering Guangdong Laboratory, Shantou, 515063, P. R. China*

[d]*School of Chemistry and Materials Science, Jiangsu Normal University, Xuzhou, 221116, China*

† Equally contributed to this work.

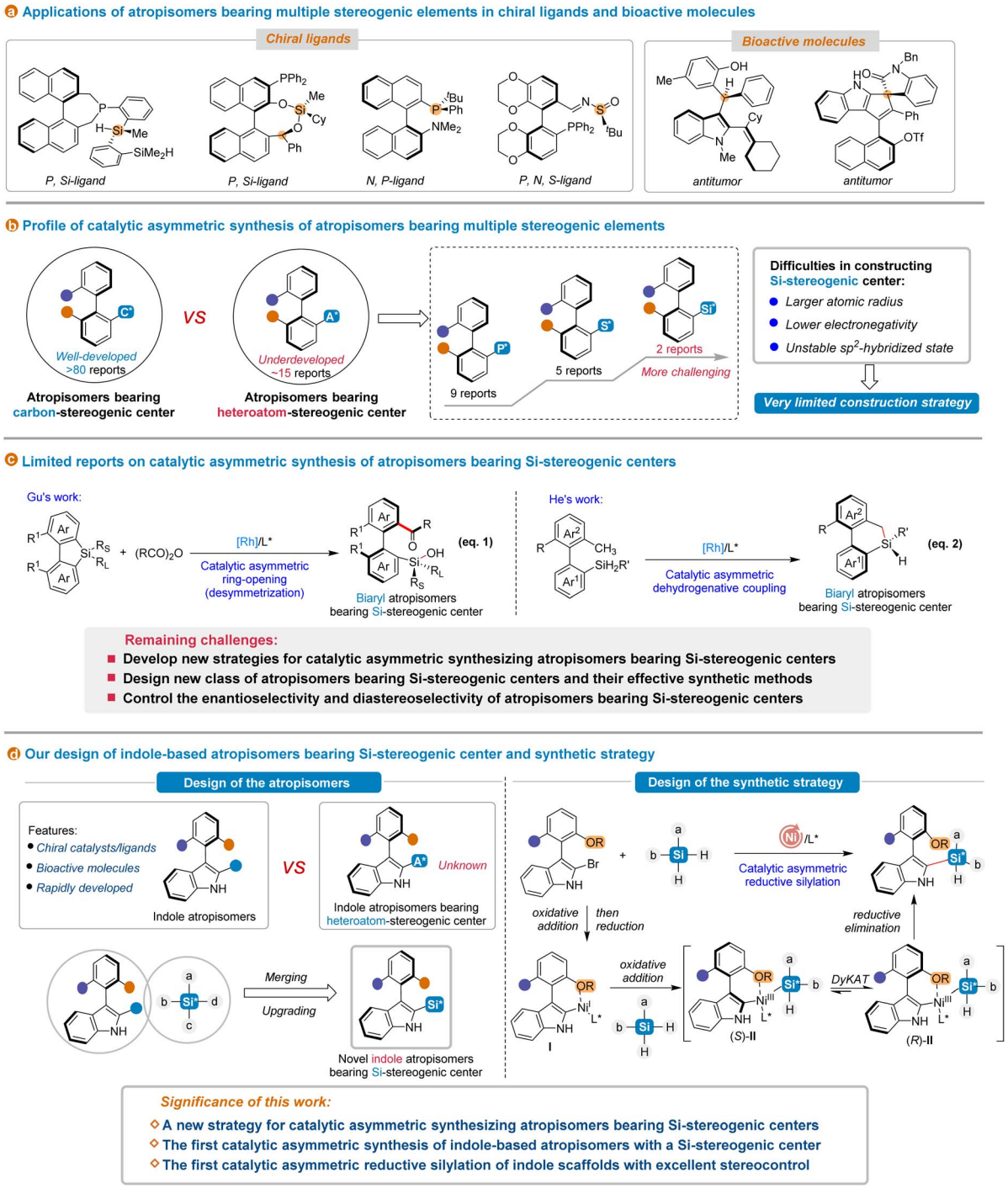

Fig. 1 Current status of catalytic asymmetric synthesis of atropisomers bearing a silicon-stereogenic center, the remaining challenges and our design.

indole-based atropisomers bearing Si-stereogenic centers (Fig. 1d). In recent years, catalytic asymmetric synthesis of indole atropisomers has become an emerging area due to their wide applications in developing chiral catalysts or ligands and discovering bioactive molecules.[15b,16,17] Although this research area developed rapidly, the catalytic asymmetric synthesis of indole atropisomers bearing heteroatom-stereogenic centers is still unknown, which might be ascribed to the formidable challenges in such transformations such as overcoming the relatively lower rotational barriers and less stable configuration of indole atropisomers, simultaneously generating indole axial chirality and heteroatom central chirality with high stereocontrol. So, to disclose this unknown chemistry, we envision merging the scaffold of axially chiral indole with Si-central chirality, thus upgrading to novel indole atropisomers bearing Si-stereogenic centers.

To realize the catalytic asymmetric synthesis of this new class of indole atropisomers bearing Si-stereogenic centers, we design a nickel/chiral ligand (L*)-catalyzed reductive silylation of 2-bromo-3-arylindoles as a new strategy toward this goal, which involves enantioselective C–Si bond formation (Fig. 1d). It should be noted that enantioselective C–Si bond formation through the strategy of catalytic asymmetric reductive silylation is rarely reported.[18] Nevertheless, we consider that the power of asymmetric Ni-catalysis[19] should provide a promising opportunity for realizing enantioselective C–Si bond formation *via* reductive silylation.

In our hypothesis (Fig. 1d), the Ni-catalyst will undergo oxidative addition with 2-bromo-3-arylindoles to generate Ni^{II} species, which will be reduced to Ni^{I} intermediates **I**. Then, the Ni^{I} intermediates will undergo another oxidative addition with silanes to give intermediates (*R*)-**II** and (*S*)-**II**, which further undergo reductive elimination to yield the designed indole atropisomers bearing Si-stereogenic centers. Notably, in the structures of Ni^{III} intermediates (*R*)-**II** and (*S*)-**II**, the low rotational barrier and weak coordination between nickel and the alkoxyl (OR) group will facilitate tautomerization between the two stereoisomers, thus realizing the dynamic kinetic asymmetric transformation (DyKAT)[20] in the reaction process and controlling the stereoselectivity of the indole atropisomers bearing Si-stereogenic centers.

Therefore, the significance of this work lies in that it will not only provide a new strategy for catalytic asymmetric synthesis of atropisomers bearing Si-stereogenic centers, but also accomplish the first catalytic asymmetric synthesis of indole-based atropisomers with a Si-stereogenic center. Moreover, this work will present the first catalytic asymmetric reductive silylation of indole scaffolds with excellent stereocontrol.

Results and discussion

With this design in mind, the reaction of 2-bromo-3-arylindole **1a** and methyl(phenyl)silane **2a** was utilized to test the possibility of our designed catalytic asymmetric reductive silylation (Table 1). As expected, indole atropisomer **3aa** bearing a Si-stereogenic center was obtained in 12% yield with 10% ee and 1.1 : 1 dr in the presence of $NiBr_2$(dme) as a Ni-catalyst, using an oxazoline ligand **L1** as a chiral ligand and Mn powder as a reductant in THF at 50 °C (entry 1). After the evaluation of different chiral oxazoline ligands **L1–L8** (entries 1–8), **L4** was found to be advantageous in stereoselectivity control (entry 4), which resulted in the generation of product **3aa** with an improved diastereo- and enantioselectivity (66% ee, 2.3 : 1 dr). Further changing the oxidation state of the nickel catalyst and its counterion did not show an evident effect on enhancing the stereoselectivity (entries 9–10 *vs.* entry 4). So, $NiBr_2$(dme) was still chosen as the suitable nickel catalyst to investigate the solvent effects (entries 11–15), which revealed that 2-MeTHF was much superior to other solvents in terms of controlling the reactivity and stereoselectivity (entry 12), affording product **3aa** in an enhanced yield and stereoselectivity (44% yield, 73% ee, 2.4 : 1 dr). Thus, 2-MeTHF was selected as the optimal solvent for further condition optimization.

Table 1 Screening catalysts and solvents for the synthesis of indole atropisomers bearing Si-stereogenic centers[a]

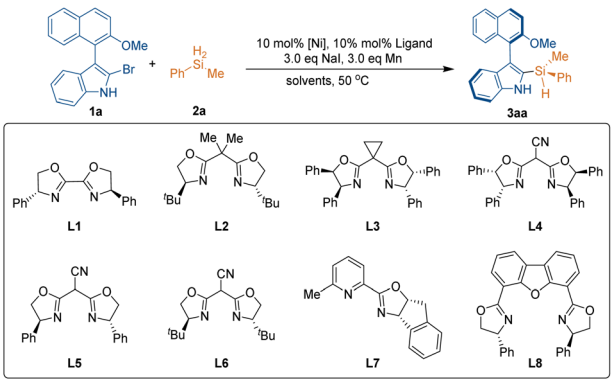

Entry	Ligand	Solvent	Yield[b] (%)	ee[c] (%)	dr[d]
1	**L1**	THF	12	−10	1.1 : 1
2	**L2**	THF	Trace	—	—
3	**L3**	THF	39	5	1.2 : 1
4	**L4**	THF	33	66	2.3 : 1
5	**L5**	THF	9	−71	2.3 : 1
6	**L6**	THF	Trace	—	—
7	**L7**	THF	41	−14	1.1 : 1
8	**L8**	THF	7	−2	1.1 : 1
9[e]	**L4**	THF	29	69	2.4 : 1
10[f]	**L4**	THF	10	65	2.5 : 1
11	**L4**	Dioxane	Trace	—	—
12	**L4**	2-MeTHF	44	73	2.4 : 1
13	**L4**	MTBE	Trace	—	—
14	**L4**	Toluene	Trace	—	—
15	**L4**	MeCN	Trace	—	—

[a] Reaction conditions: **1a** (0.1 mmol), **2a** (0.3 mmol), $NiBr_2$(dme) (0.01 mmol), ligand (0.01 mmol), NaI (0.3 mmol), Mn (0.3 mmol), and solvent (1 mL), *T* °C, 12 h. [b] Isolated yields. [c] The ee value was determined by HPLC. [d] The dr value was determined by HPLC and ^{1}H NMR. [e] $NiCl_2$(dme) was used as a catalyst. [f] Ni(cod)$_2$ was used as a catalyst.

In further study, other reaction parameters such as additives, bases and temperature were optimized (Table 2). The evaluation of different additives (entries 1–5) disclosed that using NH_4Cl as an additive instead of NaI could generate **3aa** in a higher yield with better diastereo- and enantioselectivity (entry 3 *vs.* Table 1, entry 12). Surprisingly, the addition of a stoichiometric base benefited the enantiocontrol of the chiral Ni-catalyst possibly by the neutralization of the generated HBr (entries 6–10). For example, the use of K_2CO_3 as a base afforded atropisomer **3aa** in 89% ee and 4 : 1 dr (entry 7). The subsequent variation of the reaction temperature disclosed a delicate effect on the catalytic asymmetric silylation (entries 11–13). Namely, elevating the temperature to 60 °C led to diminished stereoselectivity of product **3aa** (entry 13), whereas lowering the temperature to 40 °C boosted the diastereomeric ratio of **3aa** to 6.7 : 1 albeit with a reduced yield of 39% (entry 12). At last, to increase the yield, the reaction time was extended to 96 h, resulting in a greatly improved yield of 61% with a high enantioselectivity of 93% ee and a good diastereoselectivity of 5.6 : 1 dr (entry 14). So, the

Table 2 Further condition optimization for the synthesis of indole atropisomers bearing Si-stereogenic centers[a]

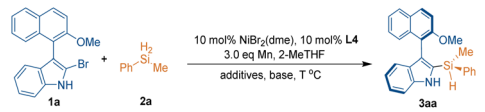

Entry	Additives	Base	Yield[b] (%)	ee[c] (%)	dr[d]
1	LiCl	—	61	78	3.1 : 1
2	KF	—	49	68	2.6 : 1
3	NH_4Cl	—	63	79	3.3 : 1
4	NaF	—	48	66	2.7 : 1
5	NaCl	—	60	69	2.6 : 1
6	NH_4Cl	Cs_2CO_3	13	84	2.9 : 1
7	NH_4Cl	K_2CO_3	45	89	4 : 1
8	NH_4Cl	Na_2CO_3	42	88	4.4 : 1
9	NH_4Cl	K_3PO_4	44	89	5.1 : 1
10	NH_4Cl	Et_3N	17	85	4.2 : 1
11[e]	NH_4Cl	K_2CO_3	12	82	6.1 : 1
12[f]	NH_4Cl	K_2CO_3	39	88	6.7 : 1
13[g]	NH_4Cl	K_2CO_3	31	84	3.8 : 1
14[f,h]	NH_4Cl	K_2CO_3	61	93	5.6 : 1

[a] Reaction conditions: **1a** (0.1 mmol), **2a** (0.3 mmol), $NiBr_2$(dme) (0.01 mmol), **L4** (0.01 mmol), additives (0.3 mmol), Mn (0.3 mmol), bases (0.2 mmol) and 2-methyltetrahydrofuran (1 mL), *T* °C, 12 h. [b] Isolated yields. [c] The ee value was determined by HPLC. [d] The dr value was determined by HPLC and ^{1}H NMR. [e] The reaction temperature is 30 °C. [f] The reaction temperature is 40 °C. [g] The reaction temperature is 60 °C. [h] The reaction time was 96 h.

conditions in entry 14 were established as the optimized conditions for the synthesis of indole atropisomers bearing Si-stereogenic centers *via* catalytic asymmetric reductive silylation.

Following the establishment of optimized reaction conditions, we evaluated the substrate compatibility of the catalytic asymmetric silylation for the synthesis of indole atropisomers bearing Si-stereogenic centers (Fig. 2). At first, the substrate scope of 2-bromo-3-arylindoles **1** was examined, and it was found that a wide range of substrates **1** were amenable to the strategy of catalytic asymmetric reductive silylation, leading to the generation of numerous indole-based atropisomers **3** bearing Si-stereogenic centers in acceptable yields (35–77%) with overall high enantioselectivities (66–94% ee) and moderate to good diastereoselectivities (1.6 : 1–7.3 : 1 dr). In detail, 3-arylindoles **1** with R^1 substituents in the C4–C5 position of the indole ring could smoothly take part in the silylation reaction to give atropisomers **3ba–3ga** in generally high enantioselectivities. Due to the C4-steric effect of the indole ring, C4-fluoro-substituted substrate **1b** exhibited much lower reactivity than others and required longer reaction time to generate product **3ba**. Moreover, C6-substituted 3-arylindoles **1h–1k** bearing alkyl, aryl, and halogen substituents served as competent substrates for the catalytic asymmetric silylation, which afforded products **3ha–3ka** bearing both indole axial chirality and Si-central chirality in generally high enantioselectivities (89–91% ee) and good diastereoselectivities (3.2 : 1–5.9 : 1 dr). Notably, electron-withdrawing substituents such as the trifluoromethyl group obviously decreased the reactivity of 3-arylindole **1l**, which participated in the reaction in a very sluggish way to generate the corresponding product **3la**. Additionally, C7-substituted 3-arylindoles **1m–1o** were also suitable coupling partners for methyl(phenyl)silane **2a**, and these reactions proceeded smoothly to give products **3ma–3oa** in a highly enantioselective manner (90–94% ee) with good diastereoselectivities (4 : 1–7.1 : 1 dr). In addition to monosubstituted 3-arylindoles, C6,C7-disubstituted 3-arylindoles were capable of undergoing the Ni-catalyzed asymmetric reductive silylation, affording atropisomers **3pa–3sa** bearing Si-stereogenic centers in moderate yields with good stereoselectivities. Furthermore, the R^2 group in the moiety of naphthalene could be changed from methoxyl to ethoxyl, and this substrate **1s** displayed similar reactivity and stereoselectivity to its analogue **1a** to give product **3sa** in 64% yield with 93% ee and 4.8 : 1 dr. Notably, 2,6-disubstituted phenyl-type substrates **1t** and **1u** smoothly participated in the catalytic asymmetric reductive silylation under standard conditions to give the corresponding products **3tf** and **3ua** in acceptable yields with moderate enantioselectivities.

Subsequently, the substrate scope of silanes **2** in the catalytic asymmetric reductive silylation reaction was explored (Fig. 2). Generally, a variety of silanes **2** bearing different Ar/R^3 substituents could serve as reliable silylating reagents toward the synthesis of indole atropisomers **3** bearing Si-stereogenic centers in a highly enantioselective manner (82–94% ee) with moderate to good diastereoselectivities (3.1 : 1–6.4 : 1 dr). Specifically, a series of Ar groups bearing either electron-donating or electron-withdrawing substituents at *ortho*-, *meta*- and *para*-positions of the phenyl ring could be utilized, and these substrates **2b–2h** smoothly underwent catalytic asymmetric reductive silylation with 2-bromo-3-arylindole **1a** to yield the desired products **3ab–3ah** in moderate to good yields with high enantiocontrol. It seemed that the existence of an *ortho*-substituent was helpful to improve the diastereoselectivity, as exemplified by substrate **2b** bearing an *ortho*-methoxy group, which afforded product **3ab** in a high diastereoselectivity of 5.0 : 1 dr. Moreover, naphthyl-substituted silanes **2i–2j** demonstrated outstanding suitability in the reaction, giving products **3ai** and **3aj** in good yields with high diastereo- and enantioselectivities. Moreover, the R^3 substituent could be changed from the methyl group to other alkyl groups such as ethyl, *n*-propyl and *t*-butyl, and these silanes **2k–2m** successfully underwent reductive silylation with 2-bromo-3-arylindole **1a** to produce indole atropisomers with multiple chiral elements in moderate yields (52–61%) with excellent stereoselectivities (90–94% ee, 4.5 : 1–6.4 : 1 dr).

To demonstrate the practicality of the catalytic asymmetric reductive silylation in the synthesis of indole-based atropisomers with a Si-stereogenic center, we performed one-mmol-scale synthesis and some transformations of product **3aa** (Scheme 1). The one-mmol-scale reaction between **1a** and **2a** smoothly afforded indole-based atropisomer **3aa** in a high yield of 90% with a good stereoselectivity of 85% ee and 3.5 : 1 dr (Scheme 1a). Furthermore, several functionalizations of the Si–H group in product **3aa** were performed through transition metal-catalyzed reactions (Scheme 1b–d). For example, Pt-

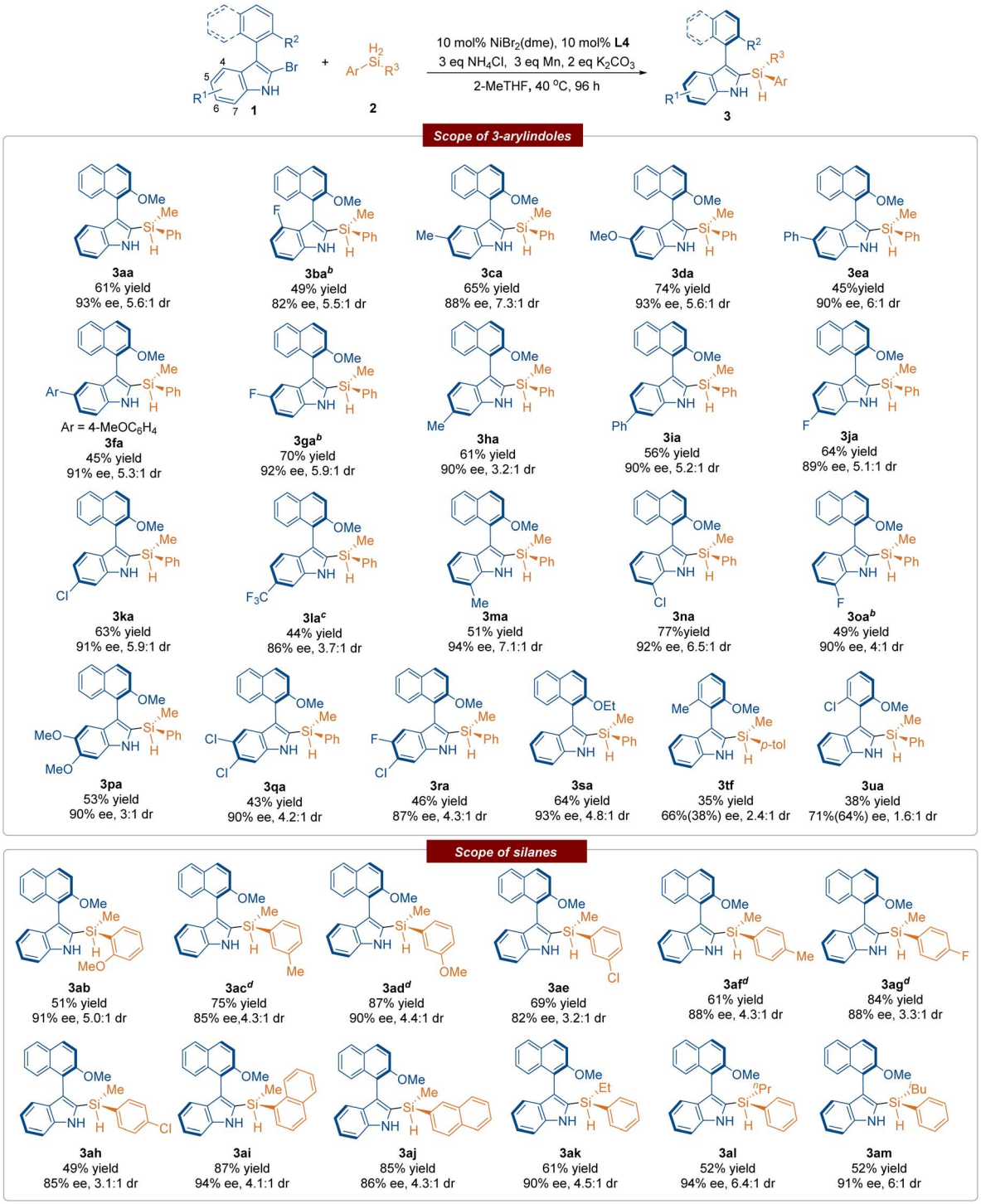

Fig. 2 Substrate scope for the synthesis of indole atropisomers bearing Si-stereogenic centers.[a] Reaction conditions: **1** (0.1 mmol), **2a** (0.3 mmol), $NiBr_2$(dme) (0.01 mmol), **L4** (0.01 mmol), NH_4Cl (0.3 mmol), Mn (0.3 mmol), K_2CO_3 (0.2 mmol) and 2-methyltetrahydrofuran (1 mL), 40 °C, 96 h, isolated yields, the ee value was determined by HPLC, the d.r. value were determined by ^1H NMR. The absolute configuration of the major diastereomer of product **3pa** was determined to be (R_a,*S*) by the X-ray diffraction analysis of its single crystal.[21] [b] The reaction was carried out for 168 h. [c] The reaction was carried out for 240 h. [d] The reaction was carried out for 144 h.

catalyzed olefination of **3aa** gave rise to axially chiral indole-based silane **4** bearing an all-carbon quaternary Si-stereogenic center (Scheme 1b). Moreover, compound **3aa** could undergo Rh-catalyzed stereoselective Si–O coupling with acetone or 4-methoxyphenol, giving products **5** and **6** *via* the formation of a Si–O bond in a nearly retained stereoselectivity (Scheme 1c and d).

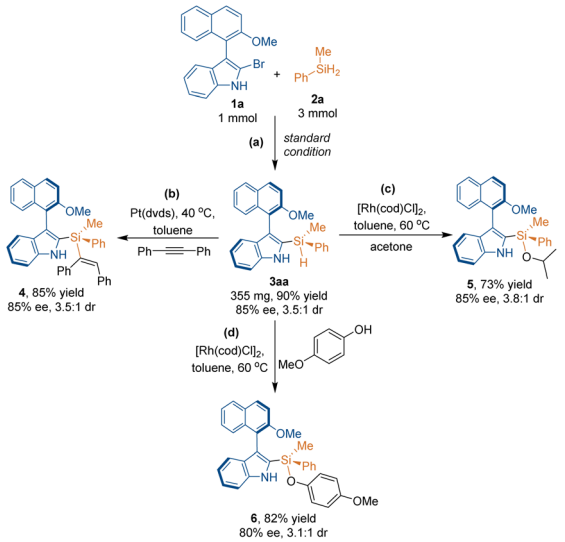

Scheme 1 One-mmol-scale reaction and downstream transformations.

Based on previous reports,[18] we proposed a mechanism for the catalytic asymmetric reductive silylation (Scheme 2a). As exemplified by the formation of product **3aa**, the transformation started from the coordination and reduction of the Ni^{II}-catalyst to generate a chiral Ni^{0}-catalyst (Ni^{0}-**L4**). Then, the oxidative addition of 2-bromo-3-arylindole **1a** to the Ni^{0}-catalyst afforded Ni^{II} intermediate **A**, which was further reduced by Mn powder to give Ni^{I} intermediates **B**. Then, the oxidative addition of silane **2a** to intermediate **B** gave Ni^{III} intermediate **C** bearing a Si-stereogenic center, which further underwent reductive elimination to afford the final indole atropisomer **3aa** with a Si-stereogenic center and release the Ni^{I} complex. The generated Ni^{I} complex was further reduced by Mn powder to regenerate the Ni^{0}-catalyst and accomplish the catalytic cycle.

To further understand the reaction pathway, we calculated the rotational barriers of substrate **1a**, intermediates **A–C** and product **3aa** by a theoretical method (Scheme 2b, see the SI for details). It was discovered that the rotational barriers of substrate **1a** and product **3aa** are much higher than the 24.0 kcal mol^{-1} required for isolating two atropisomers at room temperature, while those of intermediates **A–C** are lower than 24.0 kcal mol^{-1}. These results indicated that this reaction was not a kinetic resolution (KR) process, but a dynamic kinetic asymmetric transformation (DyKAT). Namely, due to the low rotational barrier of intermediates **A–C**, the tautomerization between the atropisomers of **A–C** and **A′–C′** could readily occur, thus facilitating the DyKAT process, and the final step of reductive elimination determined the absolute configuration of the axial chirality in product **3aa**.

To verify the proposed reaction pathway, we performed some control experiments (Scheme 3). Firstly, we subjected 2-bromo-2′-methoxy-1,1′-binaphthalene **7** (a substrate with the indole ring replaced with a naphthalene moiety) to the reaction conditions. As shown in Scheme 3a, substrate **7** failed to participate in the reductive silylation, and no reaction occurred under standard conditions. This result indicated that the indole ring is very important for the reactivity of the substrates in the catalytic asymmetric reductive silylation. To further understand the reactivity difference between substrates **7** and **1**, theoretical calculations on the rotational barriers in the reaction system of substrate **7** were conducted, including supposed intermediates **D–F** and product **8**. Unlike 2-bromo-3-arylindole **1**, the rotation in this binaphthalene system is more restricted. The DFT calculations revealed significantly high rotational barriers for substrate **7** (36.3 kcal mol^{-1}), the corresponding nickelacycle

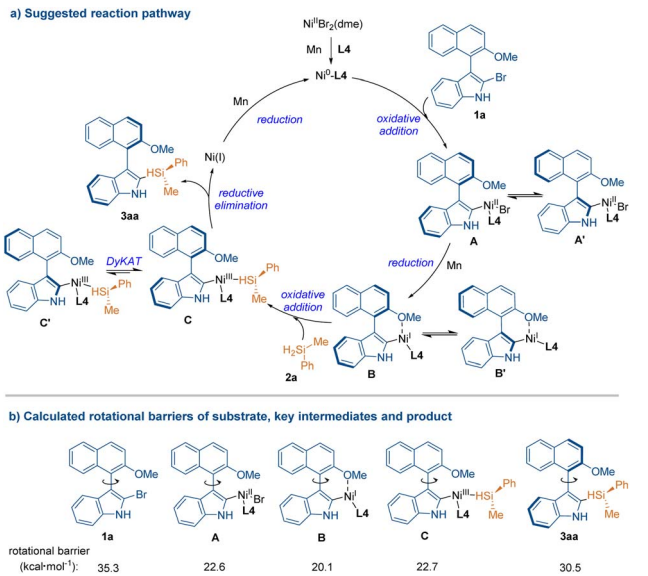

Scheme 2 Proposed reaction pathway and calculated rotational barriers.

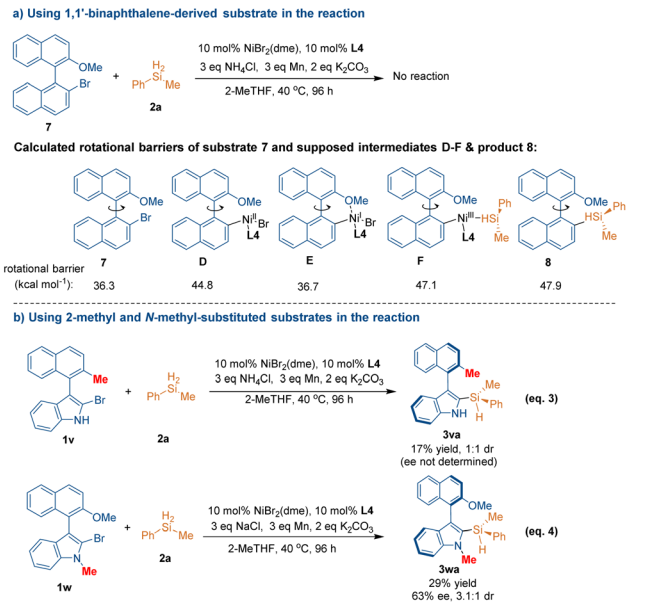

Scheme 3 Control experiments to verify the proposed reaction pathway.

intermediates **D–F** (44.8, 36.7, and 47.1 kcal mol^{-1}, respectively), and the supposed product **8** (47.9 kcal mol^{-1}). Notably, the high rotational barriers of the key intermediates **D–F** indicate that the interconversion between the atropisomers would be exceedingly slow under the catalysis of Ni/**L4**. This high configurational stability of the binaphthalene system contrasts sharply with our designed naphthyl-indole system, wherein a much lower rotational barrier is essential for the rapid equilibration between atropisomers. These computational results strongly support our observation that the unique structural features of the naphthyl-indole scaffold facilitate the DyKAT pathway.

Secondly, to demonstrate the role of the methoxy group in stabilizing or directing nickelacycle formation, the methoxy group in substrate **1** was replaced by a methyl group. As shown in Scheme 3b, under standard conditions, methyl-substituted substrate **1v** underwent Ni-catalyzed reductive silylation to give product **3va** in a low yield of 17% (eqn (3)), which supported the proposed coordination-based mechanism, *i.e.*, the coordination of the oxygen atom in the methoxy group to the nickel catalyst is crucial for the reductive silylation reaction. Moreover, we employed *N*-methyl-substituted substrate **1w** in the catalytic asymmetric reductive silylation reaction. As shown in eqn (4), this substrate **1w** could react with **2a** to give the corresponding product **3wa** in 29% yield with 63% ee and 3.1 : 1 dr. This result primarily ruled out the possibility that the observed racemization arises from tautomeric interconversion of the indole ring in one of the intermediates, involving temporary formation of an sp^3 carbon at the stereogenic axis.

Finally, to clarify the nature of the observed diastereomers, we synthesized products bearing either axial or silicon chirality and studied their configurational stability (Scheme 4a). Specifically, we utilized symmetric silane (diphenylsilane) **2n** as a substrate to synthesize product **3an** bearing only axial chirality (60% ee, eqn (5)) and employed substrate **1x** in the reductive silylation reaction to generate product **3xa** bearing only silicon chirality (55% ee, eqn (6)). Then, we conducted epimerization experiments of products **3an** and **3xa** in ^{i}PrOH at 70 °C for 12 hours. It was found that indole atropisomer **3an** underwent epimerization with a decreased ee value (32% ee), while the ee value of chiral silane **3xa** was well retained (55% ee).

Notably, in the presence of chiral ligand **L9**, substrate **1x** could undergo nickel-catalyzed asymmetric reductive silylation with **2a** to give product **3xa** bearing a silicon stereocenter in a moderate enantioselectivity of 55% ee albeit with an unsatisfactory yield of 26% (eqn (6)). By changing the additive from NH_4Cl to NH_4Br, the yield of **3xa** could be improved to 45% with a nearly retained enantioselectivity of 53% ee. So, this result indicated that this nickel-catalyzed asymmetric reductive silylation has moderate selectivity for forming the silicon stereocenter in simpler systems, and the atropisomer formation indeed assists the selectivity of the silicon stereocenter.

Furthermore, we isolated both diastereomers of **3aa** and tested whether they converge into the same diastereomeric mixture upon heating. As shown in Scheme 4b, by column chromatography (petroleum ether : acetone = 500 : 1) on silica gel, we isolated the major diastereomer of **3aa** with 11.5 : 1 dr and the minor diastereomer of **3aa** with <1 : 19 dr. Then, we conducted epimerization experiments by heating both diastereomers of **3aa** in ^{i}PrOH at 70 °C. It was found that the dr value of the major diastereomer dropped to 1.08 : 1 after 38 hours (eqn (7)), while the dr value of the minor diastereomer dropped to 1 : 1.06 after 78 hours (eqn (8)). Evidently, both diastereomers of **3aa** converged into a similar diastereomeric mixture upon heating. So, these results demonstrated that the diastereomers are epimers at the stereogenic axis.

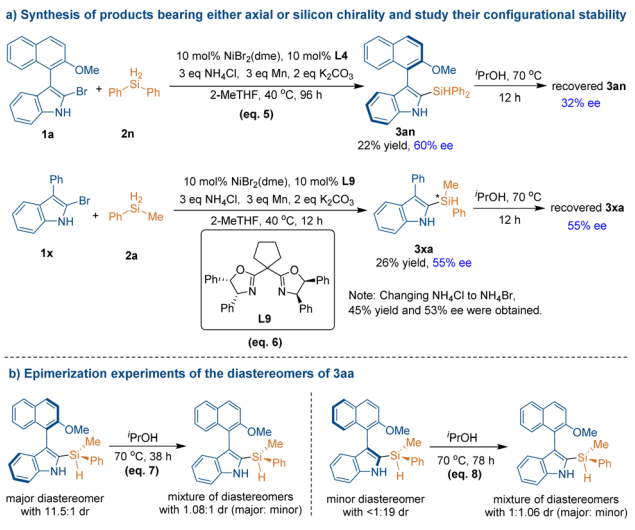

Scheme 4 Experiments to clarify the nature of the observed diastereomers.

Conclusions

In summary, we have established the first diastereo- and enantioselective synthesis of indole-based atropisomers bearing Si-stereogenic centers by the strategy of catalytic asymmetric reductive silylation of an indole scaffold in the presence of a Ni-catalyst. Through this strategy, various indole-based atropisomers bearing both axial chirality and Si-central chirality were synthesized in moderate to good yields with excellent enantioselectivities and overall good diastereoselectivities (up to 87% yield, 94% ee, 7.1 : 1 dr). Moreover, such indole-based atropisomers could be functionalized through olefination and Si–O couplings, demonstrating their promising applications. This study not only provides a new strategy for catalytic asymmetric synthesis of atropisomers bearing Si-stereogenic centers, but also has realized the first catalytic asymmetric synthesis of indole-based atropisomers with a Si-stereogenic center, which will add an important member to the family of indole-based atropisomers bearing multiple chiral elements. This study also presents the first catalytic asymmetric reductive silylation of indole scaffolds, which will serve as a good example for enantioselective C–Si bond formation.

Author contributions

Feng Shi conceived and co-supervised the project and finalized the manuscript. Zi-Qi Zhu co-supervised the project, wrote the

draft manuscript and prepared the SI. Si-Yi Liu performed the majority of the experiments. Ni–Na Feng performed some experiments. Shao-Fei Ni supervised the theoretical calculations. Fei-Xiao Chen performed theoretical calculations. All the authors proofread and commented on the manuscript.

Conflicts of interest

There are no conflicts to declare.

Data availability

The data supporting this article have been included as part of the supplementary information (SI). Supplementary information: experimental procedures, characterization data, NMR spectra, HPLC traces, and additional figures supporting the results presented in the main text. See DOI: **https://doi.org/10.1039/d5sc05320j**.

CCDC 2448426 contains the supplementary crystallographic data for this paper.

Acknowledgements

This work was supported by the National Natural Science Foundation of China (22125104 and 22401020), the Natural Science Foundation of Jiangsu Province (BK20230624) and the Guangdong Basic and Applied Basic Research Foundation (2024A1515010323 and 2025A1515011907). We also thank the Analysis and Testing Center, NERC Biomass of Changzhou University, for the assistance in NMR analysis.

Notes and references

1 For selected early reviews: (*a*) D. Bonne and J. Rodriguez, *Chem. Commun.*, 2017, **53**, 12385–12393; (*b*) D. Bonne and J. Rodriguez, *Eur. J. Org Chem.*, 2018, **2018**, 2417–2431; (*c*) Y.-B. Wang and B. Tan, *Acc. Chem. Res.*, 2018, **51**, 534–547; (*d*) G. Liao, T. Zhou, Q.-J. Yao and B.-F. Shi, *Chem. Commun.*, 2019, **55**, 8514–8523; (*e*) X. Bao, J. Rodriguez and D. Bonne, *Angew. Chem., Int. Ed.*, 2020, **59**, 12623–12634; (*f*) J. A. Carmona, C. Rodríguez-Franco, R. Fernández, V. Hornillos and J. M. Lassaletta, *Chem. Soc. Rev.*, 2021, **50**, 2968–2983; (*g*) J. K. Cheng, S.-H. Xiang, S. Li, L. Ye and B. Tan, *Chem. Rev.*, 2021, **121**, 4805–4902; (*h*) C.-X. Liu, W.-W. Zhang, S.-Y. Yin, Q. Gu and S.-L. You, *J. Am. Chem. Soc.*, 2021, **143**, 14025–14040, for a book: (*i*) B. Tan, *Axially Chiral Compounds: Asymmetric Synthesis and Applications*, VCH, Weinheim, 2021.

2 For selected recent reviews: (*a*) G.-J. Mei, W. L. Koay, C.-Y. Guan and Y. Lu, *Chem*, 2022, **8**, 1855–1893; (*b*) Y.-J. Wu, G. Liao and B.-F. Shi, *Green Synth. Catal.*, 2022, **3**, 117–136; (*c*) X. Zhang, K. Zhao and Z. Gu, *Acc. Chem. Res.*, 2022, **55**, 1620–1633; (*d*) W. Qin, Y. Liu and H. Yan, *Acc. Chem. Res.*, 2022, **55**, 2780–2795; (*e*) J. K. Cheng, S.-H. Xiang and B. Tan, *Acc. Chem. Res.*, 2022, **55**, 2920–2937; (*f*) P. Rodríguez-Salamanca, R. Fernández, V. Hornillos and J. M. Lassaletta, *Chem.–Eur. J.*, 2022, **28**, e202104442; (*g*) J. Feng, C.-J. Lu and R.-R. Liu, *Acc. Chem. Res.*, 2023, **56**, 2537–2554; (*h*) Y.-B. Chen, Y.-N. Yang, X.-Z. Huo, L.-W. Ye and B. Zhou, *Sci. China: Chem.*, 2023, **66**, 2480–2491; (*i*) S.-H. Xiang, W.-Y. Ding, Y.-B. Wang and B. Tan, *Nat. Catal.*, 2024, **7**, 483–498; (*j*) J. Feng and R.-R. Liu, *Chem.–Eur. J*, 2024, **30**, e202303165.

3 For reviews: (*a*) X.-F. Bai, Y.-M. Cui, J. Cao and L.-W. Xu, *Acc. Chem. Res.*, 2022, **55**, 2545–2561; (*b*) A. Luca and J. Wencel-Delord, *Chem. Commun.*, 2023, **59**, 8159–8167; (*c*) A. Gaucherand, E. Yen-Pon, A. Domain, A. Bourhis, J. Rodriguez and D. Bonne, *Chem. Soc. Rev.*, 2024, **53**, 11165–11206; (*d*) H.-H. Zhang, T.-Z. Li, S.-J. Liu and F. Shi, *Angew. Chem., Int. Ed.*, 2024, **63**, e202311053.

4 For selected examples: (*a*) H. Lai, Z. Huang, Q. Wu and Y. Qin, *J. Org. Chem.*, 2009, **74**, 283–288; (*b*) A. M. Taylor, R. A. Altman and S. L. Buchwald, *J. Am. Chem. Soc.*, 2009, **131**, 9900–9901; (*c*) L. Chen, J.-B. Huang, Z. Xu, Z.-J. Zheng, K.-F. Yang, Y.-M. Cui, J. Cao and L.-W. Xu, *RSC Adv.*, 2016, **6**, 67113–67117; (*d*) B. Yang, J. Gao, X. Tan, Y. Ge and C. He, *Angew. Chem., Int. Ed.*, 2023, **62**, e202307812.

5 For selected examples: (*a*) S. Yang, J.-B. Huang, D.-H. Wang, N.-Y. Wang, Y.-Y. Chen, X.-Y. Ke, H. Chen, S.-F. Ni, Y.-C. Zhang and F. Shi, *Precis. Chem.*, 2024, **2**, 208–220; (*b*) P. Wu, W.-T. Zhang, J.-X. Yang, X.-Y. Yu, S.-F. Ni, W. Tan and F. Shi, *Angew. Chem., Int. Ed.*, 2024, **63**, e202410581.

6 For selected examples of biaryl atropisomers bearing carbon-stereogenic centers: (*a*) T. Saget and N. Cramer, *Angew. Chem., Int. Ed.*, 2013, **52**, 7865–7868; (*b*) V. Hornillos, J. A. Carmona, A. Ros, J. Iglesias-Sigüenza, J. López-Serrano, R. Fernández and J. M. Lassaletta, *Angew. Chem., Int. Ed.*, 2018, **57**, 3777–3781; (*c*) J. A. Carmona, V. Hornillos, P. Ramírez-López, A. Ros, J. Iglesias-Sigüenza, E. Gómez-Bengoa, R. Fernández and J. M. Lassaletta, *J. Am. Chem. Soc.*, 2018, **140**, 11067–11075; (*d*) S. Lu, J.-Y. Ong, H. Yang, S. B. Poh, X. Liew, C. S. D. Seow, M. W. Wong and Y. Zhao, *J. Am. Chem. Soc.*, 2019, **141**, 17062–17067; (*e*) D. Liang, J.-R. Chen, L.-P. Tan, Z.-W. He and W.-J. Xiao, *J. Am. Chem. Soc.*, 2022, **144**, 6040–6049; (*f*) J.-Y. Du, T. Balan, T. D. W. Claridge and M. D. Smith, *J. Am. Chem. Soc.*, 2022, **144**, 14790–14797; (*g*) L. Dai, X. Zhou, J. Guo, X. Dai, Q. Huang and Y. Lu, *Nat. Commun.*, 2023, **14**, 4813; (*h*) H. Jiang, X.-K. He, X. Jiang, W. Zhao, L.-Q. Lu, Y. Cheng and W.-J. Xiao, *J. Am. Chem. Soc.*, 2023, **145**, 6944–6952; (*i*) A. Domain, X. Bao, J. Rodriguez and D. Bonne, *Chem.–Eur. J.*, 2024, **30**, e202403374; (*j*) Z.-J. Zhang, N. Jacob, S. Bhatia, P. Boos, X. Chen, J. C. DeMuth, A. M. Messinis, B. B. Jei, J. C. A. Oliveira, A. Radović, M. L. Neidig, J. Wencel-Delord and L. Ackermann, *Nat. Commun.*, 2024, **15**, 3503; (*k*) J. Moon, E. Shin and Y. Kwon, *J. Am. Chem. Soc.*, 2025, **147**, 12800–12810.

7 For selected examples of nonbiaryl atropisomers bearing carbon-stereogenic centers: (*a*) N. D. Iorio, P. Righi, A. Mazzanti, M. Mancinelli, A. Ciogli and G. Bencivenni, *J. Am. Chem. Soc.*, 2014, **136**, 10250–10253; (*b*) C. Min, Y. Lin and D. Seidel, *Angew. Chem., Int. Ed.*, 2017, **56**, 15353–15357; (*c*) J. Bie, M. Lang and J. Wang, *Org. Lett.*, 2018, **20**, 5866–5871; (*d*) X.-W. Gu, Y.-L. Sun, J.-L. Xie, X.-B. Wang,

Z. Xu, G.-W. Yin, L. Li, K.-F. Yang and L.-W. Xu, *Nat. Commun.*, 2020, **11**, 2904; (*e*) F. Sun, T. Wang, G.-J. Cheng and X. Fang, *ACS Catal.*, 2021, **11**, 7578–7583; (*f*) F. Wang, J. Jing, Y. Zhao, X. Zhu, X.-P. Zhang, L. Zhao, P. Hu, W.-Q. Deng and X. Li, *Angew. Chem., Int. Ed.*, 2021, **60**, 16628–16633; (*g*) B.-B. Gou, Y. Tang, Y.-H. Lin, L. Yu, Q.-S. Jian, H.-R. Sun, J. Chen and L. Zhou, *Angew. Chem., Int. Ed.*, 2022, **61**, e202208174; (*h*) R. Mi, Z. Ding, S. Yu, R. H. Crabtree and X. Li, *J. Am. Chem. Soc.*, 2023, **145**, 8150–8162; (*i*) T. v. Münchow, Y.-R. Liu, R. Parmar, S. E. Peters, S. Trienes and L. Ackermann, *Angew. Chem., Int. Ed.*, 2024, **63**, e202405423; (*j*) X. Li, X.-Z. Wang, B. Shen, Q.-Y. Chen, H. Xiang, P. Yu and P.-N. Liu, *Nat. Commun.*, 2025, **16**, 1662; (*k*) J. Gu, L.-H. Zhang, H.-F. Zhuang and Y. He, *Chem. Sci.*, 2025, **16**, 5735–5744.

8 For catalytic asymmetric synthesis of atropisomers bearing P-stereogenic centers: (*a*) Y.-S. Jang, Ł. Woźniak, J. Pedroni and N. Cramer, *Angew. Chem., Int. Ed.*, 2018, **57**, 12901–12905; (*b*) P. Hu, L. Kong, F. Wang, X. Zhu and X. Li, *Angew. Chem., Int. Ed.*, 2021, **60**, 20424–20429; (*c*) D. Ji, J. Jing, Y. Wang, Z. Qi, F. Wang, X. Zhang, Y. Wang and X. Li, *Chem*, 2022, **8**, 3346–3362; (*d*) C.-W. Zhang, X.-Q. Hu, Y.-H. Dai, P. Yin, C. Wang and W.-L. Duan, *ACS Catal.*, 2022, **12**, 193–199; (*e*) L. Pang, Q. Sun, Z. Huang, G. Li, J. Liu, J. Guo, C. Yao, J. Yu and Q. Li, *Angew. Chem., Int. Ed.*, 2022, **61**, e202211710; (*f*) L. Pang, Z. Huang, Q. Sun, G. Li, J. Liu, B. Li, C. Ma, J. Guo, C. Yao, J. Yu and Q. Li, *Nat. Commun.*, 2023, **14**, 4437; (*g*) B. Jiang, H. Wang, X. Sun, Y. Qiao, X. Xu and Z. Miao, *Adv. Synth. Catal.*, 2025, **367**, e202500021; (*h*) R. Cui, Y. Zhang, Z. Huang, L. Yuwen, Y. Xu and Q.-W. Zhang, *Angew. Chem., Int. Ed.*, 2024, **63**, e202412064; (*i*) S. Gao, L. Su and J. Liu, *J. Am. Chem. Soc.*, 2025, **147**, 23946–23956.

9 For catalytic asymmetric synthesis of atropisomers bearing S-stereogenic centers:(*a*) J. Clayden and H. Turner, *Tetrahedron Lett.*, 2009, **50**, 3216–3219; (*b*) G. Zheng, X. Li and J.-P. Cheng, *Org. Lett.*, 2021, **23**, 3997–4001; (*c*) Y. Chang, C. Xie, H. Liu, S. Huang, P. Wang, W. Qin and H. Yan, *Nat. Commun.*, 2022, **13**, 1933; (*d*) W. Wen, C.-L. Yang, Z.-L. Wu, D.-R. Xiao and Q.-X. Guo, *Adv. Sci.*, 2024, **11**, 2402429; (*e*) W. Fang, Y.-D. Meng, S.-Y. Ding, J.-Y. Wang, Z.-H. Pei, M.-L. Shen, C.-Z. Yao, Q. Li, Z. Gu, J. Yu and H.-J. Jiang, *Angew. Chem., Int. Ed.*, 2025, **64**, e202419596.

10 For catalytic asymmetric synthesis of atropisomers bearing Si-stereogenic centers: (*a*) X. Bi, J. Feng, X. Xue and Z. Gu, *Org. Lett.*, 2021, **23**, 3201–3206; (*b*) Y. Guo, M.-M. Liu, X. Zhu, L. Zhu and C. He, *Angew. Chem., Int. Ed.*, 2021, **60**, 13887–13891.

11 During the preparation of this manuscript, another elegant report appeared but with only three examples on constructing Si-stereogenic centers: H.-J. Zhu, M.-H. Shen, J.-W. Si, W.-K. Zhu, X.-J. Fang, F. Ye, J. Cao, Z. Xu and L.-W. Xu, *Sci. China: Chem.*, 2025, **68**, 2513–2523.

12 For reviews on enantioselective construction of Si-stereogenic centers: (*a*) L.-W. Xu, L. Li, G.-Q. Lai and J.-X. Jiang, *Chem. Soc. Rev.*, 2011, **40**, 1777–1790; (*b*) Y.-M. Cui, Y. Lin and L.-W. Xu, *Coord. Chem. Rev.*, 2017, **330**, 37–52; (*c*) W. Yuan and C. He, *Synthesis*, 2022, **54**, 1939–1950; (*d*) W.-S. Huang, Q. Wang, H. Yang and L.-W. Xu, *Synthesis*, 2022, **54**, 5400–5408; (*e*) L. Li, W.-S. Huang, Z. Xu and L.-W. Xu, *Sci. China: Chem.*, 2023, **66**, 1654–1687; (*f*) Y. Ge, J. Ke and C. He, *Acc. Chem. Res.*, 2025, **58**, 375–398; (*g*) Y. Ge, X. Huang, J. Ke and C. He, *Chem Catal.*, 2022, **2**, 2898–2928.

13 For early examples on enantioselective construction of Si-stereogenic centers: (*a*) K. Tamao, K. Nakamura, H. Ishii, S. Yamaguchi and M. Shiro, *J. Am. Chem. Soc.*, 1996, **118**, 12469–12470; (*b*) Y. Yasutomi, H. Suematsu and T. Katsuki, *J. Am. Chem. Soc.*, 2010, **132**, 4510–4511; (*c*) R. Shintani, K. Moriya and T. Hayashi, *J. Am. Chem. Soc.*, 2011, **133**, 16440–16443; (*d*) Y. Kurihara, M. Nishikawa, Y. Yamanoi and H. Nishihara, *Chem. Commun.*, 2012, **48**, 11564–11566; (*e*) K. Igawa, D. Yoshihiro, N. Ichikawa, N. Kokan and K. Tomooka, *Angew. Chem., Int. Ed.*, 2012, **51**, 12745–12748; (*f*) R. Shintani, H. Otomo, K. Ota and T. Hayashi, *J. Am. Chem. Soc.*, 2012, **134**, 7305–7308.

14 For recent examples on enantioselective construction of Si-stereogenic centers: (*a*) X.-C. Wang, B. Li, C.-W. Ju and D. Zhao, *Nat. Commun.*, 2022, **13**, 3392; (*b*) W. Yuan, X. Zhu, Y. Xu and C. He, *Angew. Chem., Int. Ed.*, 2022, **61**, e202204912; (*c*) Y. Zeng, X.-J. Fang, R.-H. Tang, J.-Y. Xie, F.-J. Zhang, Z. Xu, Y.-X. Nie and L.-W. Xu, *Angew. Chem., Int. Ed.*, 2022, **61**, e202214147; (*d*) M.-M. Liu, Y. Xu and C. He, *J. Am. Chem. Soc.*, 2023, **145**, 11727–11734; (*e*) W.-E. Gan, Y.-S. Wu, B. Wu, C.-Y. Fang, J. Cao, Z. Xu and L.-W. Xu, *Angew. Chem., Int. Ed.*, 2024, **63**, e202317973; (*f*) Y. Shi, Y. Qin, Z.-Q. Li, Y. Xu, S. Chen, J. Zhang, Y.-A. Li, Y. Wu, F. Meng, Y.-W. Zhong and D. Zhao, *Angew. Chem., Int. Ed.*, 2024, **63**, e202405520; (*g*) T. Hu, Y. Zhang, W. Wang, Q. Li, L. Huang, J. Gao, Y. Kuang, C. Zhao, S. Zhou, L. Gao, Z. Su and Z. Song, *J. Am. Chem. Soc.*, 2024, **146**, 23092–23102; (*h*) X. Tang, Y. Tang, J. Peng, H. Du, L. Huang, J. Gao, S. Liu, D. Wang, W. Wang, L. Gao, Y. Lan and Z. Song, *J. Am. Chem. Soc.*, 2024, **146**, 26639–26648; (*i*) J.-H. Zhao, L. Zheng, J.-Y. Zou, S.-Y. Zhang, H.-C. Shen, Y. Wu and P. Wang, *Angew. Chem., Int. Ed.*, 2024, **63**, e202402612; (*j*) F.-H. Gou, F. Ren, Y. Wu and P. Wang, *Angew. Chem., Int. Ed.*, 2024, **63**, e202404732.

15 For summaries: (*a*) Y.-C. Zhang, F. Jiang and F. Shi, *Acc. Chem. Res.*, 2020, **53**, 425–446; (*b*) H.-H. Zhang and F. Shi, *Acc. Chem. Res.*, 2022, **55**, 2562–2580, for recent examples: (*c*) J.-Y. Wang, C.-H. Gao, C. Ma, X.-Y. Wu, S.-F. Ni, W. Tan and F. Shi, *Angew. Chem., Int. Ed.*, 2024, **63**, e202316454; (*d*) T. Li, S. Liu, S. Wu, Q. Cheng, Q. Chen, Y. Jiao, Y. Zhang and F. Shi, *Sci. China: Chem.*, 2024, **67**, 2629–2636; (*e*) N.-Y. Wang, S. Gao, Z.-D. Shu, B.-B. Cheng, C. Ma, Y.-C. Zhang and F. Shi, *Sci. China: Chem.*, 2025, **68**, 3130–3137.

16 For reviews: (*a*) T.-Z. Li, S.-J. Liu, W. Tan and F. Shi, *Chem.–Eur. J.*, 2020, **26**, 15779–15792; (*b*) J. Wei, M. Zhu, B. Zhang, K. Li and X. Zhang, *Tetrahedron*, 2023, **149**, 133716; (*c*) J. Wang, Z. Wang, W. Hea and L. Ye, *Chin. J. Org. Chem.*, 2024, **44**, 1786–1792.

17 For recent examples: (*a*) Z.-S. Wang, L.-J. Zhu, C.-T. Li, B.-Y. Liu, X. Hong and L.-W. Ye, *Angew. Chem., Int. Ed.*, 2022, **61**, e202201436; (*b*) S. Jia, Y. Tian, X. Li, P. Wang, Y. Lan and H. Yan, *Angew. Chem., Int. Ed.*, 2022, **61**, e202206501; (*c*) L.-W. Zhan, C.-J. Lu, J. Feng and R.-R. Liu, *Angew. Chem., Int. Ed.*, 2023, **62**, e202312930; (*d*) W. Yao, C.-J. Lu, L.-W. Zhan, Y. Wu, J. Feng and R.-R. Liu, *Angew. Chem., Int. Ed.*, 2023, **62**, e202218871; (*e*) S.-Y. Yin, Q. Zhou, C.-X. Liu, Q. Gu and S.-L. You, *Angew. Chem., Int. Ed.*, 2023, **62**, e202305067; (*f*) Y.-H. Chen, M. Duan, S.-L. Lin, Y.-W. Liu, J. K. Cheng, S.-H. Xiang, P. Yu, K. N. Houk and B. Tan, *Nat. Chem.*, 2024, **16**, 408–416; (*g*) W. Bao, Y.-H. Chen, Y.-W. Liu, S.-H. Xiang and B. Tan, *Chin. J. Chem.*, 2024, **42**, 731–735; (*h*) H.-H. Chen, Y.-B. Chen, J.-Z. Gao, L.-W. Ye and B. Zhou, *Angew. Chem., Int. Ed.*, 2024, **63**, e202411709; (*i*) C. Song, C. Pang, Y. Deng, H. Cai, X. Gan and Y. R. Chi, *ACS Catal.*, 2024, **14**, 6926–6935; (*j*) R. Mi, R. Wu, J. Jing, F. Wang, X.-X. Li, X. Hong and X. Li, *Sci. Adv.*, 2024, **10**, eadr4435; (*k*) J. Wang, D. Pan, F. Wang, S. Yu, G. Huang and X. Li, *Sci. Adv.*, 2024, **10**, eado4489.

18 For limited examples of enantioselective C-Si bond formation *via* reductive silylation: (*a*) L. Wang, W. Lu, J. Zhang, Q. Chong and F. Meng, *Angew. Chem., Int. Ed.*, 2022, **61**, e202205624; (*b*) L. Qi, Q.-Q. Pan, X.-X. Wei, X. Pang, Z. Liu and X.-Z. Shu, *J. Am. Chem. Soc.*, 2023, **145**, 13008–13014.

19 For recent examples of asymmetric Ni-catalysis: (*a*) Y. Zhang, D. Qiao, M. Duan, Y. Wang and S. Zhu, *Nat. Commun.*, 2022, **13**, 5630; (*b*) C. Zhang, X. Wu, T. Xia, J. Qu and Y. Chen, *Nat. Commun.*, 2022, **13**, 5964; (*c*) L. Huo, X. Li, Y. Zhao, L. Li and L. Chu, *J. Am. Chem. Soc.*, 2023, **145**, 9876–9885; (*d*) L. Lu, S. Chen, W. Kong, B. Gao, Y. Li, L. Zhu and G. Yin, *J. Am. Chem. Soc.*, 2024, **146**, 16639–16647; (*e*) Z. Zhou, Y. Ke, R. Miao, F. Hu, X. Wang, Y. Ping, S. Xu and W. Kong, *Nat. Chem.*, 2025, **17**, 344–355; (*f*) G.-Y. Han, P.-F. Su, Q.-Q. Pan, X.-Y. Liu and X.-Z. Shu, *Nat. Catal.*, 2024, **7**, 12–20; (*g*) X.-Y. Chen, Q. Yu and W. Shu, *Angew. Chem., Int. Ed.*, 2025, **64**, e202423426; (*h*) X. Fang, L. Xi, M. Wang, J. Xiao, Y. Zhao, M. C. Willis and Z. Shi, *Nat. Commun.*, 2025, **16**, 2547.

20 For examples of using DyKAT strategies for the synthesis of biaryl atropisomers involving the formation of metallacyclic intermediates, for Pd catalysis: (*a*) J. A. Carmona, V. Hornillos, P. Ramirez-Lopez, A. Ros, J. Iglesias-Sigüenza, E. Gómez-Bengoa, R. Fernańdez and J. M. Lassaletta, *J. Am. Chem. Soc.*, 2018, **140**, 11067–11075; (*b*) Y.-W. Sun, J.-H. Zhao, X.-Y. Yan, C.-L. Ji, H. Feng and D.-W. Gao, *Nat. Commun.*, 2024, **15**, 10810; (*c*) Y. Xiao, A. L. Bartelt, E. Irran and M. Oestreich, *ACS Catal.*, 2025, **15**, 11307–11312; (*d*) S. Gao, L. Su and J. Liu, *J. Am. Chem. Soc.*, 2025, **147**, 23946–23956; (*e*) B. Ye, L. Su, K. Zheng, S. Gao and J. Liu, *Angew. Chem., Int. Ed.*, 2025, **64**, e202413949; for Co catalysis: (*f*) X. Jiang, W. Xiong, S. Deng, F.-D. Lu, Y. Jia, Q. Yang, L.-Y. Xue, X. Qi, J. A. Tunge, L.-Q. Lu and W.-J. Xiao, *Nat. Catal.*, 2022, **5**, 788–797; (*g*) W. Xiong, X. Jiang, W.-C. Wang, Y. Cheng, L.-Q. Lu, K. Gao and W.-J. Xiao, *J. Am. Chem. Soc.*, 2023, **145**, 7983–7991; (*h*) C. Lin, X. Xu, Q. Chong and F. Meng, *Chem.–Eur. J.*, 2025, **31**, e202500248; for Ni catalysis: (*i*) T. Sun, Z. Zhang, Y. Su, H. Cao, Y. Zhou, G. Luo and Z.-C. Cao, *J. Am. Chem. Soc.*, 2023, **145**, 15721–15728; (*j*) X.-W. Chen, C. Li, Y.-Y. Gui, J.-P. Yue, Q. Zhou, L.-L. Liao, J.-W. Yang, J.-H. Ye and D.-G. Yu, *Angew. Chem., Int. Ed.*, 2024, **63**, e202403401.

21 CCDC 2448426 for compound **3pa**, 2025, DOI: **10.5517/ccdc.csd.cc2n5sh4**.